Chinese Journal of
POLYMER SCIENCE

RESEARCH ARTICLE

https://doi.org/10.1007/s10118-024-3211-8
Chinese J. Polym. Sci.

Photoswitchable Spiropyridine Enabled Photoactuation of Polymeric Hydrogels under Physiological pH Conditions

Cong Liao, Meng-Qi Du, and Chuang Li*

Key Laboratory of Precision and Intelligent Chemistry, Department of Polymer Science and Engineering, University of Science and Technology of China, Anhui 230026, China

Electronic Supplementary Information

Abstract The incorporation of molecular switches into polymer networks has been a powerful approach for the development of functional polymer materials that display macroscopic actuation and function enabled directly by molecular changes. However, such materials sometimes require harsh conditions to perform their functions, and the design of new molecular photoswitches that can function under physiological conditions is highly needed. Here, we report the design and synthesis of a spiropyridine-based photoswitchable hydrogel that exhibits light-driven actuation at physiological pH. Owing to its high pK_a, spiropyridine maintains its ring-open protonated form at neutral pH, and the resulting hydrogel remains in a swollen state. Upon irradiation with visible light, the ring closure of spiropyridine leads to a decrease in the charge and a reduction in the volume of the hydrogel. The contracted gel could spontaneously recover to its expanding state in the dark, and this process is highly dynamic and reversible when the light is switched on and off. Furthermore, the hydrogel shows switchable fluorescence in response to visible light. Bending deformation is observed in the hydrogel thin films upon irradiation from one side. Importantly, the independence of this spiropyridine hydrogel from the acidic environment makes it biotolerant and shows excellent biocompatibility. This biocompatible spiropyridine hydrogel might have important biorelated applications in the future.

Keywords Spiropyridine photowitch; Polymer hydrogel; Photoactuation; Physiological pH; Biocompatibility

Citation: Liao, C.; Du, M. Q.; Li, C. Photoswitchable spiropyridine enabled photoactuation of polymeric hydrogels under physiological pH conditions. *Chinese J. Polym. Sci*. https://doi.org/10.1007/s10118-024-3211-8

INTRODUCTION

Hydrogels are an important class of soft materials composed of crosslinked hydrophilic polymers and a high content of water.[1,2] Due to their structural and mechanical similarity to the natural extracellular matrix,[3] hydrogels have attracted considerable attention in different areas for widespread applications, such as biomedical[4] and tissue engineering,[5] artificial muscles,[6,7] and soft robotics.[8,9] In particular, stimuli-responsive hydrogels are capable of changing their chemical or physical properties, such as shape,[10,11] color[12] and stiffness,[13] in response to external stimuli, enabling them a high flexibility and adaptivity,[14,15] which are critical for maintaining their structure and function for survival and evolution. Among various physical and chemical stimuli, light[16] is particularly unique and useful due to its noninvasive delivery and high spatiotemporal controllability, allowing precise on-demand regulation of the microstructures and macroscopic properties of hydrogels. To date, photoresponsive hydrogels have been developed through different approaches,[17,18] relying on either the heating effect of integrated photothermal agents[19] or the photoisomerization of grafted molecular switches,[20,21] as well as photoinduced reversible[22] or irreversible reactions.[23] Owing to their robust reversibility and biofriendly irradiation conditions, molecular photoswitches have been broadly explored and applied for the functionalization of polymer hydrogels, endowing them with dynamic reconfigurability and adaptivity controlled by light. Recent iconic examples in this area include photoswitchable supramolecular hydrogels[24] mediated by host-guest complexation between cyclodextrin and azobenzene,[25] photoresponsive polymer hydrogels induced by diarylethenes,[26,27] spiropyran[28] and molecular motors.[29]

Despite advances in photoswitchable hydrogels, some challenges still exist on the way forward to real-world applications. One critical challenge is how to eliminate the reliance on harsh conditions for such hydrogels to perform their functions. For example, although spiropyran hydrogels have shown great potential in light-driven artificial muscles,[30] walkers,[31] actuators[32] and soft robotics,[33] they require acidic conditions to maintain the protonation of the phenol group of the ring-open merocyanine form, which greatly limits their potential biorelated applications. Therefore, the design and incorporation of photoresponsive compounds into

* Corresponding author, E-mail: lichuang21@ustc.edu.cn

Special Issue: Dynamic Polymer Networks
Received June 20, 2024; Accepted July 20, 2024; Published online August 27, 2024

hydrogels to enable them to work under biofriendly physiological conditions are highly needed. To achieve this goal, researchers have successfully designed spiropyran-based metastable photoacids[34–36] by replacing salicylaldehyde with other aromatic indazole rings that can hold a proton under physiological pH conditions. These metastable photoacids[37,38] can work in PBS buffers but have never been explored for the functionalization of polymer hydrogels. In this work, we report the molecular design and synthesis of a new polymerizable spiropyridine compound with a high pK_a that was covalently incorporated into polymer hydrogels through a free-radical copolymerization strategy. Owing to the high pK_a and reversible ring open-close isomerization of spiropyridine, the hydrogels can undergo light-driven actuation under physiological pH conditions, generating a volumetric contraction or phototropic bending deformation depending on the specific irradiation direction. Furthermore, the spiropyridine hydrogels exhibit photoswitchable fluorescence and excellent cytocompatibility, opening an avenue for future applications in cell manipulation and tissue engineering.

EXPERIMENTAL

The experimental procedures and details are described in the electronic supplementary information (ESI).

RESULTS AND DISCUSSION

Synthesis of Spiropyridine with a High pK_a

To obtain target photoswitches that function under neutral physiological conditions, the pK_a of traditional spiropyran photoswitches must be increased. To achieve this goal, we designed and synthesized a spiropyridine photoswitch that contains an indazole ring instead of a phenol ring (see Scheme S1 and Figs. S1–S3 in ESI for synthetic details). Previous work has shown that replacement of the phenol by the indazole ring effectively increased its pK_a value in metastable-state photoacids.[37,39] In our system, a polymerizable methylacrylamide group was also designed for subsequent covalent attachment to the polymer network. As shown in Fig. 1(a), the spiropyridine compound is expected to display a ring-open form in the dark and a ring-closed form upon irradiation with visible light, along with the release of a proton. We used UV-Vis absorbance spectra to further investigate the photoisomerization process in aqueous PBS buffer (pH 7.4). As shown in Fig. 1(b), the solution of the ring-open isomer exhibited a yellow color, which corresponds to a characteristic absorbance peak at 409 nm. This characteristic peak was widely observed in the UV-Vis absorbance spectra of both spiropyridine small molecules (Fig. S4 in ESI) and spiropyridine-grafted copolymers (Fig. S5 in ESI) under various acidic and neutral conditions. These results indicated that the ring-open isomer was the dominant isomer present over a wide range of pH values. Upon irradiation with blue light, the peak disappeared, and the yellow color faded, which could be attributed to the formation of the colorless ring-closed isomer. Fitting the photoisomerization kinetic curves to the ExpDec1 function gave a photoisomerization rate of 0.102 s^{-1} in PBS buffer (pH 7.4) and 0.085 s^{-1} in DI water (Fig. S6 in ESI). Importantly, the ring-closed isomer spontaneously isomerized to the thermodynamically stable ring-open form upon irradiation was switched off (Fig. 1c). The spontaneous ring-opening rates were calculated to be 0.04 s^{-1} in PBS buffer (pH 7.4) and 0.016 s^{-1} in DI water (Fig. S7 in ESI), respectively. By alternating light switching on and off, the isomerization between the ring-closed and ring-open forms is highly reversible, and the isomerization can be cycled for multiple cycles without obvious performance decay in PBS buffer (pH 7.4) (Fig. 1d) or in DI water (Fig. S8 in ESI).

Furthermore, we systematically investigated the photoacidity of spiropyridine in dilute aqueous environments at variable pH values using UV-Vis absorption spectra by probing its dark equilibrium composition (Fig. 1e). A kinetic plot of the characteristic absorbance of the ring-open form (409 nm) was fitted to Bolzmann's sigmoidal equation,[40,41] as shown in Fig. 1(f), giving a pK_a value of 7.66. This value is very close to the physiological pH in living organisms. In comparison, we synthesized a conventional spiropyran compound whose pK_a was determined to be 4.25 (Fig. 1g) following the same protocol described above. This control spiropyran compound exhibited similar photoisomerization and thermal relaxation rates comparable to those of spiropyridine (Figs. S9 and S10 in ESI). Because its pK_a was apparently lower than the physiological pH, this control compound tended to maintain its dominant ring-closed form in PBS buffer (Fig. S11 in ESI). In addition, the aqueous solution containing spiropyridine emitted yellow fluorescence in both DI water (Fig. 2a and Fig. S12 in ESI) and PBS buffer (Fig. 2b), which could be attributed to the long-range conjugated structure of the ring-open merocyanine form. Upon irradiation with blue light, the fluorescence intensity decreased due to the light-induced ring closure of the merocyanine, which is in good agreement with the decrease in the UV-Vis absorbance intensity (Fig. S5 in ESI). Spiropyridine was also covalently incorporated into cross-linked polymer networks *via* aqueous free-radical polymerization in the presence of *N*-isopropylacrylamide monomers, *N*,*N*′-methylene bis(acrylamide) cross-linkers and ammonium persulfate/tetramethylethylenediamine initiators (see ESI for synthetic details). The spiropyridine-functionalized hydrogels were found to display photoswitchable fluorescence in response to blue light irradiation (Figs. 2c and 2d), where systems with a greater pH facilitate a greater degree of photoswitching sensitivity in both aqueous solution (Fig. S13 in ESI) and in hydrogels (Fig. S14 in ESI). As a control, no fluorescence was observed in either solution or hydrogel samples of spiropyran with a pK_a of 4.25 (Fig. S15 in ESI). These results verified that we indeed obtained a spiropyridine photoswitch with a high pK_a and therefore was able to maintain its normal photoactivity under physiological pH.

Photoactuation of Spiropyridine Hydrogels under Physiological pH

In addition to investigating the photoswitchable fluorescence of the spiropyridine hydrogels, we further explored their volumetric changes in response to light under physiological pH conditions. According to our design illustrated in Fig. 3(a), spiropyridine maintains its thermodynamically stable protonated ring-open form under physiological pH due to its relatively high pK_a, resulting in a total net charge of +1. The presence of such a positive charge makes the polymer chains hydrophilic, and the hydrogel maintains a swollen state. However, light irradiation trig-

https://doi.org/10.1007/s10118-024-3211-8

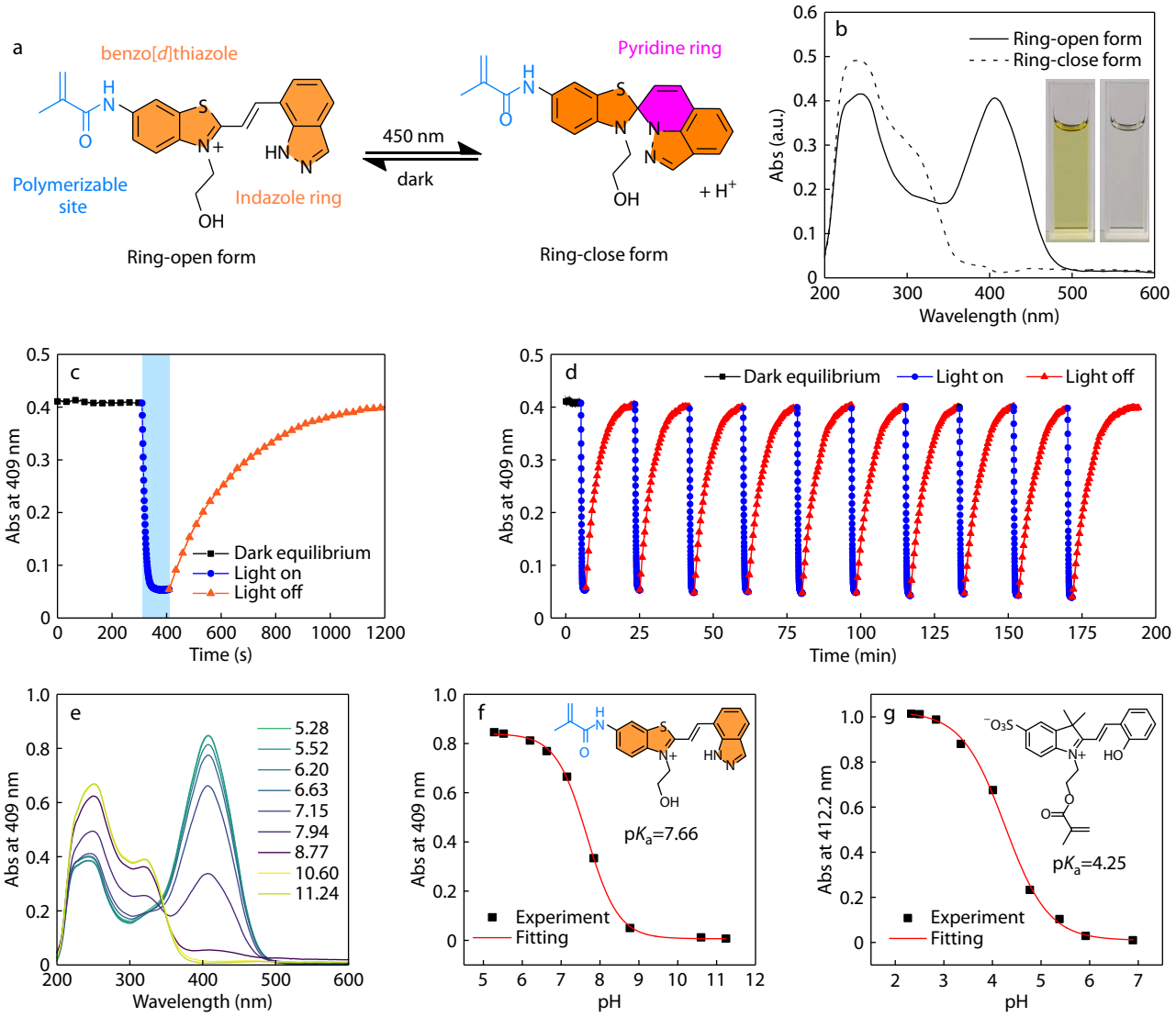

Fig. 1 Design of a polymerizable spiropyridine compound with a high pK_a. (a) Chemical structures of the ring-open (left) and ring-close (right) forms of spiropyridine before and after irradiation; (b) UV-Vis spectra of spiropyridine in PBS buffer (pH 7.4) before (solid line) and after (dashed line) irradiation with 450 nm (3 mW/cm^2). Insets are photographs of the solution before (left) and after (right) irradiation in the cuvettes. (c) Plot of the characteristic absorption of spiropyridine at 409 nm after equilibration in the dark (black), followed by switching the light on (blue) and off (red); (d) Changes in the characteristic absorption of spiropyridine at 409 nm upon alternating light switching on and off for ten cycles; (e) Equilibrated UV-Vis spectra of spiropyridine (0.05 mmol/L) in the dark at various pH values; (f) Plot and Boltzmann fitting of the absorbance of the ring-open form of spiropyridine at 409 nm as a function of pH, showing a pK_a of 7.66; (g) Plot and Boltzmann fitting of the absorbance of the control compound at 412 nm as a function of pH, which yielded a pK_a of 4.25.

gers the ring-closing isomerization of spiropyridine to become a neutrally charged and relatively hydrophobic compound, leading to macroscopic photocontraction of the hydrogel. In our experiments, we indeed observed a 20% volume contraction of the hydrogel upon irradiation with blue light (Fig. 3b). This phenomenon is in good agreement with our previous study on spiropyran hydrogels.[42–44] However, we are now able to perform such photoactuation under physiological pH conditions and do not rely on an acidic environment. As a control, the conventional spiropyran hydrogel with a low pK_a of 4.25 only works in an acidic environment (Fig. S16 in ESI) and was not able to undergo any light-driven volumetric changes under the same physiological pH conditions (Fig. S17 in ESI). To gain more insight into the microstructural changes in the hydrogel, we performed SEM experiments, as shown in Fig. 3(c) and Fig. S18 (in ESI). In agreement with the observed volume change of the hydrogels, we observed a clear decrease in the pore size of the contracted hydrogels. Inspired by phototaxis in plants, we sought to develop a series of phototactic hydrogels based on photocontraction-induced deformation in neutral water. As shown on the left in Fig. 3(d), the spiropyridine hydrogel strip is irradiated by light from the top, which creates a transient contraction gradient throughout the thickness due to stepwise light penetration. This inhomogeneous gradient generates a bending deformation toward the light source. However, with prolonged irradiation, light penetrates the hydrogel strip homogenously, resulting in a flattening deformation. We indeed observed a bending-flattening deformation of the spiropyridine

https://doi.org/10.1007/s10118-024-3211-8

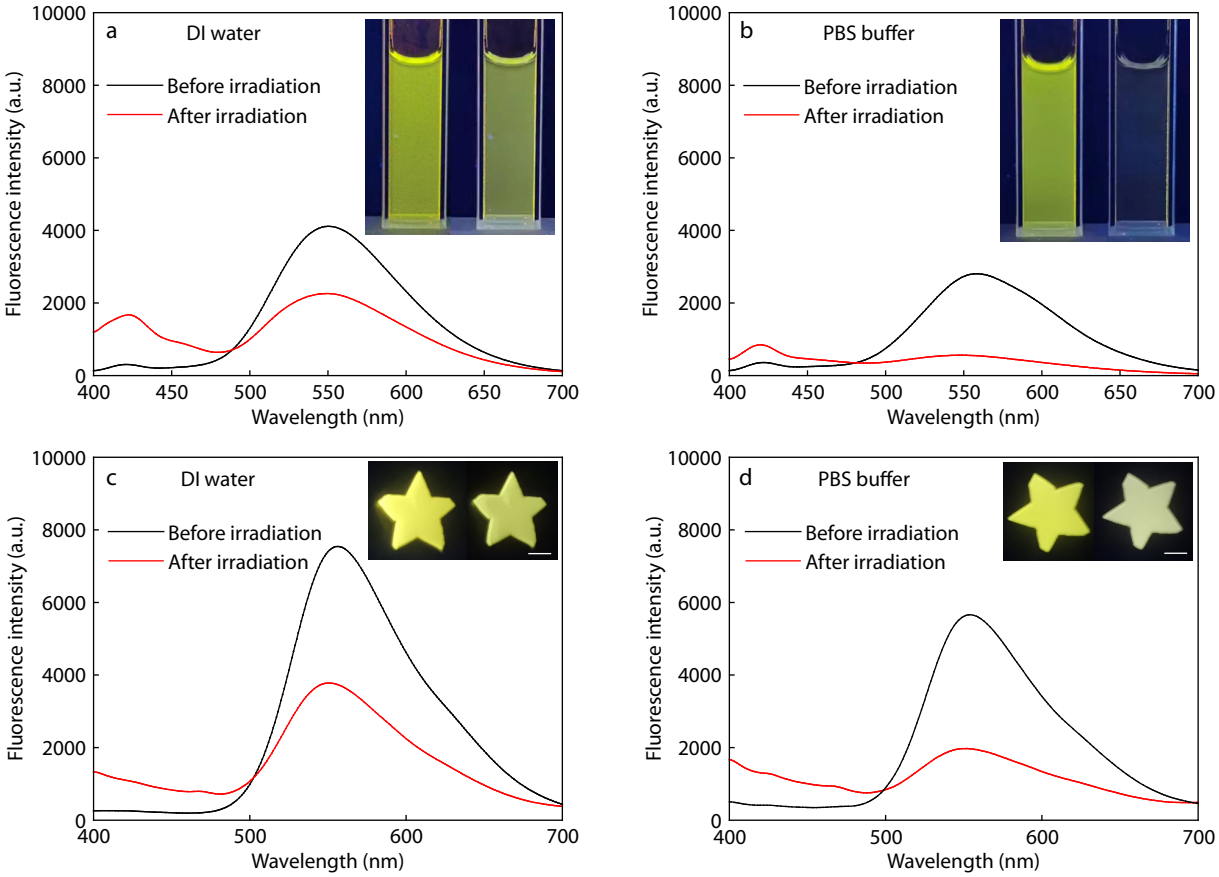

Fig. 2 Fluorescence spectra of spiropyridine (0.05 mmol/L) in (a) DI water and (b) PBS buffer (pH 7.4) before (black) and after (red) irradiation with 450 nm. Insets are photographs of the solutions in the cuvettes before and after irradiation. Fluorescence spectra of spiropyridine hydrogels equilibrated in (c) DI water and (d) PBS buffer (pH 7.4) before (black) and after (red) irradiation with 450 nm. Insets are photographs of the star-shaped hydrogels before and after irradiation. The scale bar is 5 mm.

hydrogel under physiological conditions (Fig. 3d, right), as indicated by the bending kinetics quantified by the bending angle as a function of the irradiation time, which displayed a maximum bending angle in 30 min (Fig. 3e). Noted that enhance light intensity and reduce hydrogel thickness both adverse to photoactuation due to light penetration. Reduced light intensity and increased hydrogel thickness will cause light to only act on the surface of the material which is not conducive to the formation of gradient volume change.[40] In addition, we also observed an increase in the hydrogel modulus after light exposure due to the photocontraction behavior of the gel in both DI water and PBS buffer at a pH of 7.4 (Fig. 3f).

Biocompatibility of the Spiropyridine Hydrogel

Because our spiropyridine hydrogel is able to function under physiological pH conditions, we further investigated its biocompatibility as a cell culture matrix. In our experiments, 3T3 cells were used as model cells and cultured on the hydrogel surface for 24 h, followed by a fluorescent live/dead viability assay (see ESI for details). Similar to the blank sample (culture medium without hydrogel), the presence of spiropyridine hydrogel did not lead to obvious death of cells, and most cells maintained their round uniform morphology (Fig. 4a). The quantification of live/dead stained cells revealed a cell viability as high as 98%. Furthermore, MTT (absorption at 570 nm) experiments were carried out to further test the cytotoxicity of our hydrogels at various incubation concentrations. As shown in Fig. 4(b), we consistently observed high cell viability regardless of the concentration, indicating good cytocompatibility of our hydrogels. In addition to the cytocompatibility of our spiropyridine hydrogel, we further tested its blood compatibility by incubation with blood cells for 1 h, followed by quantification of the hemolysis rate. As shown in Fig. 1(c), the hemolysis rates of blood cells incubated with different samples were obtained by measuring their absorbance change at 576 nm using an enzyme-linked immunosorbent assay. The hemolysis ratio of our spiropyridine hydrogel was approximately 2.76%, which is close to that of the negative sample incubated in PBS buffer and much lower than that of the positive sample incubated in DI water. Taken together, these results verified that our spiropyridine hydrogel not only has good cytocompatibility but also exhibits good blood compatibility, opening the possibility for future biorelated applications.

CONCLUSIONS

In summary, we synthesized a polymerizable and photoswitchable spiropyridine compound, and the thermodynamically stable ring-open isomer exhibited a high pK_a of 7.66, allowing photoisomerization in response to visible light occur at physiologi-

https://doi.org/10.1007/s10118-024-3211-8

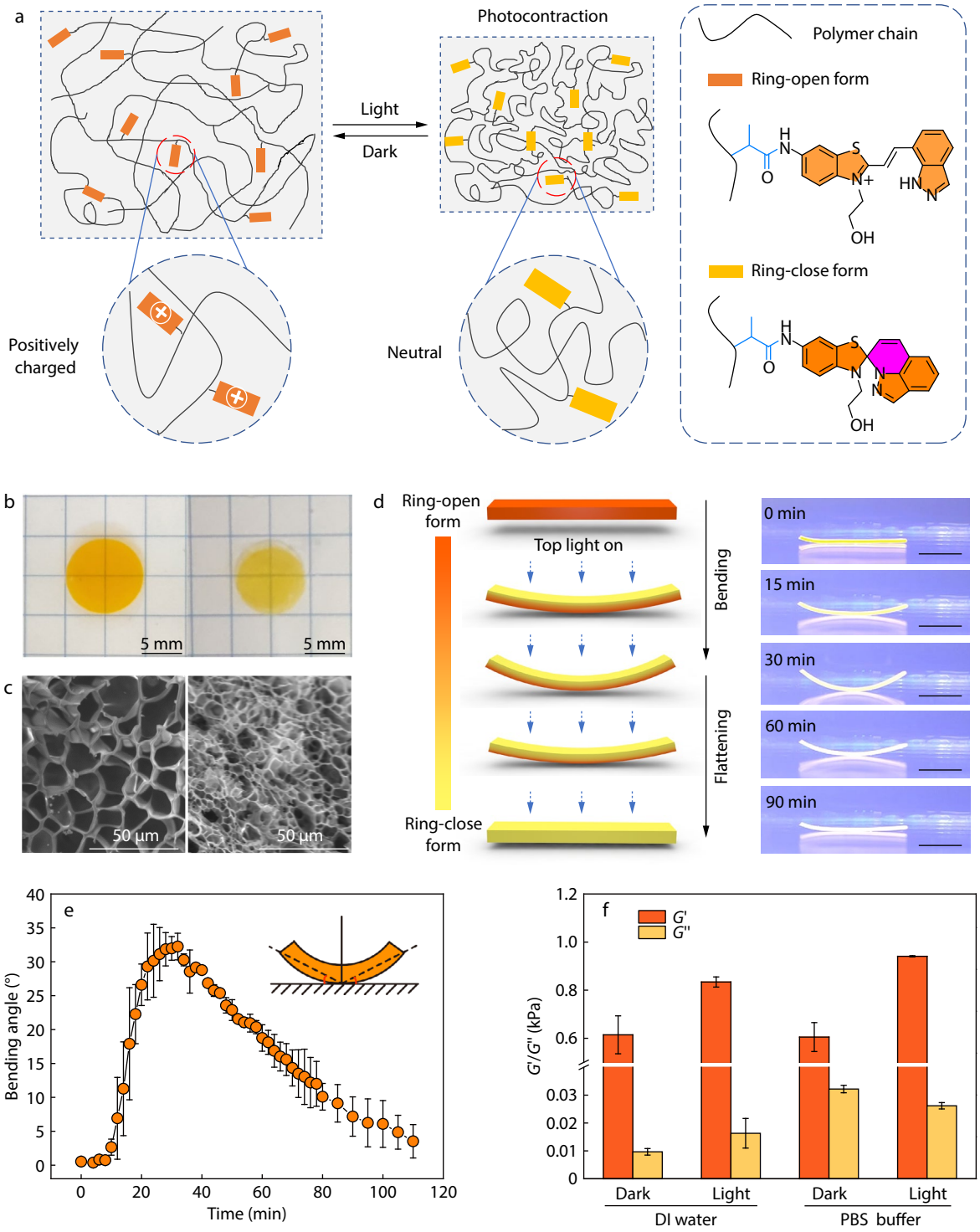

Fig. 3 (a) Schematic representation of the photontraction behavior of spiropyridine-hydrogel in response to blue light irradiation; (b) Photographs of the hydrogel before (left) and after (right) light irradiation; (c) SEM images of spiropyridine-hydrogel showing the changes in microporosity before (left) and after (right) irradiation. (d) Left, schematic representation of the bending deformation of the spiropyridine-hydrogel thin film upon irradiation from the top; right, photographs of the bending hydrogel films (0.5 mm thick) for various irradiation times using blue light (3 mW/cm^2). The scale bar is 1 cm. (e) Plot of the bending angle of the hydrogel film as a function of irradiation time. Inset is a cartoon showing the definition of bending angle. (f) Rheological measurements of spiropyridine hydrogels before and after irradiation with blue light (3 mW/cm^2). Error bars represent standard deviations of data collected from three separate samples.

https://doi.org/10.1007/s10118-024-3211-8

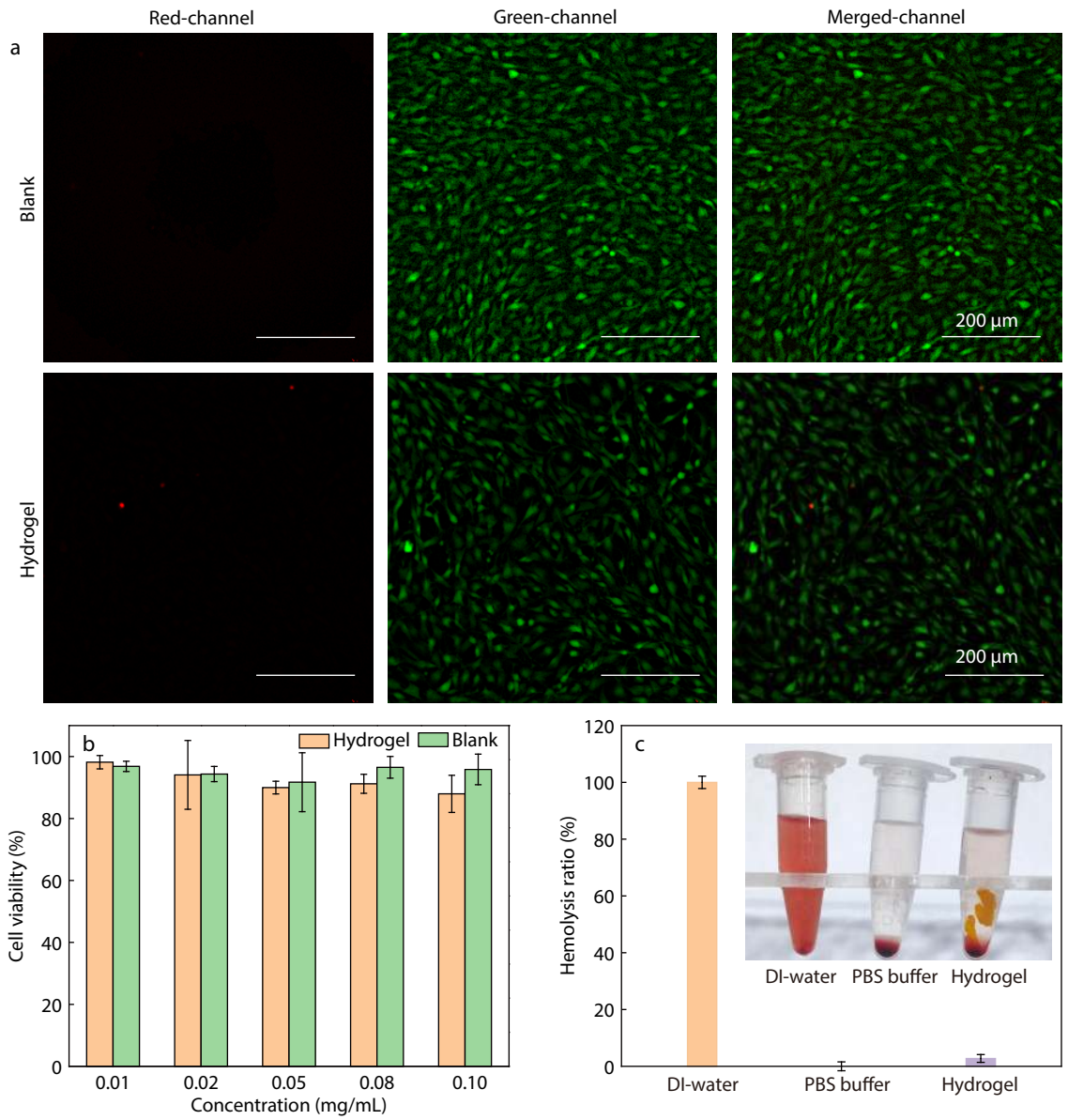

Fig. 4 (a) Fluorescent confocal microscopy images of 3T3 cells stained with both propidium iodide (PI, red) and calcein AM (green) after cocultivation with spiropyridine hydrogels for 24 h. Red and green represent dead and live cells, respectively. The blank was the cell culture medium without hydrogel. (b) Cell viability of 3T3 cells after 24 h of culture in media supplemented with various concentrations of spiropyridine-hydrogel (experiment) or saline (blank). Error bars represent standard deviations of data collected from three separate samples. (c) Plot of the hemolysis rate of the spiropyridine hydrogel incubated in PBS buffer (pH 7.4) for 1 h (experiment), PBS buffer (negative control) and DI water (positive control). Insets are images of blood cells incubated in different samples for 1 h.

cal pH. Upon covalent functionalization to a crosslinked polymer network as a pendent, the resultant spiropyridine-hydrogel displays a light-driven volume contraction under physiological pH due to the ring-closure-induced decrease in charge and hydrophilicity. In addition to reversible volume contraction-expansion, the hydrogel exhibited photoswitchable fluorescence. Furthermore, spiropyridine hydrogel thin films exhibited light-controlled bending-flattening deformation under physiological pH conditions. Most importantly, the spiropyridine-hydrogel maintains its photoactuation capability at physiological pH while being biocompatible with cells, which opens up the possibility for more complex biorelated applications in the future. We anticipate that our work will advance a step toward building a good connection between soft robotic materials and biomedical applications.

Conflict of Interests

The authors declare no interest conflict.

Electronic Supplementary Information

Electronic supplementary information (ESI) is available free of charge in the online version of this article at http://doi.org/

10.1007/s10118-024-3211-8.

Data Availability Statement

The data that support the findings of this study are available within this article (and its Supplementary Information files).

ACKNOWLEDGMENTS

This work was financially supported by the National Natural Science Foundation of China (No. 52373121), the National Key R&D Program of China (No. 2022YFA1305100) and the Natural Science Foundation of Anhui Province (No. 2208085MB27).

REFERENCES

1 Quan, H.; Kisailus, D.; Meyers, M. A. Hydration-induced reversible deformation of biological materials. *Nat. Rev. Mater.* **2020**, *6*, 264−283.
2 Kulbay, M.; Wu, K. Y.; Truong D.; Tran, S. D. Smart molecules in ophthalmology: hydrogels as responsive systems for ophthalmic applications. *Smart molecules* **2024**, *2*, e20230021.
3 Yuk, H.; Wu, J.; Zhao, X. Hydrogel interfaces for merging humans and machines. *Nat. Rev. Mater.* **2022**, *7*, 935−952.
4 Thambi, T.; Jung, J. M.; Lee, D. S. Recent strategies to develop ph-sensitive injectable hydrogels. *Biomater. Sci.* **2023**, *11*, 1948−1961.
5 Guo, B.; Liang, Y.; Dong, R. Physical dynamic double-network hydrogels as dressings to facilitate tissue repair. *Nat. Protoc.* **2023**, *18*, 3322−3354.
6 Chen, S.; Yang, L.; Leung, F. K.-C.; Kajitani, T.; Stuart, M. C. A.; Fukushima, T.; van Rijn, P.; Feringa, B. L. Photoactuating artificial muscles of motor amphiphiles as an extracellular matrix mimetic scaffold for mesenchymal stem cells. *J. Am. Chem. Soc.* **2022**, *144*, 3543−3553.
7 Matsuda, T.; Kawakami, R.; Namba, R.; Nakajima, T.; Gong, J. P. Mechanoresponsive self-growing hydrogels inspired by muscle training. *Science* **2019**, *363*, 504−508.
8 Zhao, Y.; Xuan, C.; Qian, X.; Alsaid, Y.; Hua, M.; Jin, L.; He, X. Soft phototactic swimmer based on self-sustained hydrogel oscillator. *Sci. Rob.* **2019**, *4*, eaax7112.
9 Jiao, D.; Zhu, Q. L.; Li, C. Y.; Zheng, Q.; Wu, Z. L. Programmable morphing hydrogels for soft actuators and robots: from structure designs to active functions. *Acc. Chem. Res.* **2022**, *55*, 1533−1545.
10 Liu, X.; Gao, M.; Chen, J.; Guo, S.; Zhu, W.; Bai, L.; Zhai, W.; Du, H.; Wu, H.; Yan, C.; Shi, Y.; Gu, J.; Qi, H. J.; Zhou, K. Recent advances in stimuli-responsive shape-morphing hydrogels. *Adv. Funct. Mater.* **2022**, *32*, 2203323.
11 Zhang, Y.; Liu, K.; Liu, T.; Ni, C.; Chen, D.; Guo, J.; Liu, C.; Zhou, J.; Jia, Z.; Zhao, Q.; Pan, P.; Xie, T. Differential diffusion driven far-from-equilibrium shape-shifting of hydrogels. *Nat. Commun.* **2021**, *12*, 6155.
12 Sun, Y.; Le, X.; Zhou, S.; Chen, T. Recent progress in smart polymeric gel-based information storage for anti-counterfeiting. *Adv. Mater.* **2022**, *34*, 2201262.
13 Gevorkian, A.; Morozova, S. M.; Kheiri, S.; Khuu, N.; Chen, H.; Young, E.; Yan, N.; Kumacheva, E. Actuation of three-dimensional-printed nanocolloidal hydrogel with structural anisotropy. *Adv. Funct. Mater.* **2021**, *31*, 2010743.
14 Hu, L.; Chee, P. L.; Sugiarto, S.; Yu, Y.; Shi, C.; Yan, R.; Yao, Z.; Shi, X.; Zhi, J.; Kai, D.; Yu, H. D.; Huang, W. Hydrogel-based flexible electronics. *Adv. Mater.* **2023**, *35*, 2205326.
15 Zhou, S. W.; Yu, C.; Chen, M.; Shi, C. Y.; Gu, R.; Qu, D. H. Self-healing and shape-shifting polymers controlled by dynamic bonds. *Smart Molecules* **2023**, *1*, e20220009.
16 Li, Q.; Schenning, A. P. H. J.; Bunning, T. J. Light-responsive smart soft matter technologies. *Adv. Opt. Mater.* **2019**, *7*, 1901160.
17 Li, L.; Scheiger, J. M.; Levkin, P. A. Design and applications of photoresponsive hydrogels. *Adv. Mater.* **2019**, *31*, 1807333.
18 Cong, L.; Chuang, L. Molecular design of photoresponsive hydrogels for biomimetic actuation. *J. Funct. Polym.* **2023**, *36*, 185−202.
19 Zheng, Y.; Li, C. Photothermally driven oxazine hydrogel actuators at the water-air interface. *Giant* **2023**, *16*, 100192.
20 Goulet-anssens, A.; Eisenreich, F.; Hecht, S. Enlightening materials with photoswitches. *Adv. Mater.* **2020**, *32*, 1905966.
21 Li, C.; Kazem-Rostami, M.; Seale, J. S. W.; Zhou, S.; Stupp, S. I. Macroscopic actuation of bisazo hydrogels driven by molecular photoisomerization. *Chem. Mater.* **2023**, *35*, 3923−3930.
22 Shang, H.; Le, X.; Sun, Y.; Shan, F.; Wu, S.; Zheng, Y.; Li, D.; Guo, D.; Liu, Q.; Chen, T. Integrating photorewritable fluorescent information in shape-emory organohydrogel toward dual encryption. *Adv. Opt. Mater.* **2022**, *10*, 2200608.
23 Cao, J.; Zhang, D.; Zhou, Y.; Zhang, Q.; Wu, S. Controlling properties and functions of polymer gels using photochemical reactions. *Macromol. Rapid Commun.* **2022**, *43*, 2100703.
24 Xu, F.; Feringa, B. L. Photoresponsive supramolecular polymers: from light-ontrolled small molecules to smart materials. *Adv. Mater.* **2023**, *35*, 2204413.
25 Iwaso, K.; Takashima, Y.; Harada, A. Fast response dry-type artificial molecular muscles with [c2]daisy chains. *Nat.Chem.* **2016**, *8*, 625−632.
26 Gu, Y.; Alt, E. A.; Wang, H.; Li, X.; Willard, A. P.; Johnson, J. A. Photoswitching topology in polymer networks with metal-organic cages as crosslinks. *Nature* **2018**, *560*, 65−69.
27 Li, Z. Y.; Liu, Y. Y.; Li, Y. J.; Wang, W.; Song, Y.; Zhang, J.; Tian, H. High-preservation single-cell operation through a photoresponsive hydrogel-nanopipette system. *Angew. Chem. Int. Ed.* **2021**, *60*, 5157−5161.
28 Ziółkowski, B.; Florea, L.; Theobald, J.; Benito-Lopez, F.; Diamond, D. Self-protonating spiropyran-*co*-nipam-*co*-acrylic acid hydrogel photoactuators. *Soft Matter* **2013**, *9*, 8754.
29 Chen, J.; Leung, F. K. C.; Stuart, M. C. A.; Kajitani, T.; Fukushima, T.; van der Giessen, E.; Feringa, B. L. Artificial muscle-like function from hierarchical supramolecular assembly of photoresponsive molecular motors. *Nat. Chem.* **2017**, *10*, 132−138.
30 Li, C.; Iscen, A.; Palmer, L. C.; Schatz, G. C.; Stupp, S. I. Light-driven expansion of spiropyran hydrogels. *J. Am. Chem. Soc.* **2020**, *142*, 8447−8453.
31 Li, C.; Lau, G. C.; Yuan, H.; Aggarwal, A.; Dominguez, V. L.; Liu, S.; Sai, H.; Palmer, L. C.; Sather, N. A.; Pearson, T. J.; Freedman, D. E.; Amiri, P. K.; Cruz, M. O. d. l.; Stupp, S. I. Fast and programmable locomotion of hydrogel-metal hybrids under light and magnetic fields. *Sci. Robot.* **2020**, *5*, eabb9822.
32 Hu, Y.; Ji, Q.; Huang, M.; Chang, L.; Zhang, C.; Wu, G.; Zi, B.; Bao, N.; Chen, W.; Wu, Y. Light-driven self-oscillating actuators with phototactic locomotion based on black phosphorus heterostructure. *Angew. Chem. Int. Ed.* **2021**, *60*, 20511−20517.
33 Li, C.; Xue, Y.; Han, M.; Palmer, L. C.; Rogers, J. A.; Huang, Y.; Stupp, S. I. Synergistic photoactuation of bilayered spiropyran hydrogels for predictable origami-like shape change. *Matter* **2021**, *4*, 1377−1390.
34 Liao, Y. Design and applications of metastable-state photoacids. *Acc. Chem. Res.* **2017**, *50*, 1956−1964.
35 Elgattar, A.; Alghazwat, O.; Brown, A. B.; Bryantsev, V. S.; Bocharova, V.; Liao, Y. Photoreaction of indazole metastable-state photoacid. *J. Photoch. Photobio. A* **2023**, *439*, 114599.

36 Premadasa, U. I.; Bocharova, V.; Miles, A. R.; Stamberga, D.; Belony, S.; Bryantsev, V. S.; Elgattar, A.; Liao, Y.; Damron, J. T.; Kidder, M. K.; Doughty, B.; Custelcean, R.; Ma, Y. Z. Photochemically driven CO_2 release using a metastable-state photoacid for energy efficient direct air capture. *Angew. Chem. Int. Ed.* **2023**, *62*, e202304957.
37 Abeyrathna, N.; Liao, Y. A reversible photoacid functioning in PBS buffer under visible light. *J. Am. Chem. Soc.* **2015**, *137*, 11282–11284.
38 Elgattar, A.; Abeyrathna, N.; Liao, Y. Localized pH pulses in pbs buffer repeatedly induced by visible light. *J. Phys. Chem. B* **2019**, *123*, 648–654.
39 Alghazwat, O.; Elgattar, A.; Alharithy, H.; Liao, Y. A reversible photoacid switched by different wavelengths of light. *ChemPhotoChem* **2021**, *5*, 376–380.
40 Li, C.; Iscen, A.; Sai, H.; Sato, K.; Sather, N. A.; Chin, S. M.; Álvarez, Z.; Palmer, L. C.; Schatz, G. C.; Stupp, S. I. Supramolecular-covalent hybrid polymers for light-activated mechanical actuation. *Nat. Mater.* **2020**, *19*, 900–909.
41 Berton, C.; Busiello, D. M.; Zamuner, S.; Solari, E.; Scopelliti, R.; Fadaei-Tirani, F.; Severin, K.; Pezzato, C. Thermodynamics and kinetics of protonated merocyanine photoacids in water. *Chem. Sci.* **2020**, *11*, 8457.
42 Wimberger, L.; Prasad, S. K. K.; Peeks, M. D.; Andréasson, J.; Schmidt, T. W.; Beves, J. E. Large, tunable, and reversible pH changes by merocyanine photoacids. *J. Am. Chem. Soc.* **2021**, *143*, 20758.
43 Yang, X.; Shi, W.; Chen, Z.; Du, M.; Xiao, S.; Qu, S.; Li, C. Light-fueled nonequilibrium and adaptable hydrogels for highly tunable autonomous self-oscillating functions. *Adv. Funct. Mater.* **2023**, *33*, 2214394.
44 Guo, K.; Yang, X.; Zhou, C.; Li, C. Self-regulated reversal deformation and locomotion of structurally homogenous hydrogels subjected to constant light illumination. *Nat. Commun.* **2024**, *15*, 1694.

https://doi.org/10.1007/s10118-024-3211-8